

October 1998

IFP-763-UNC

Aspects of Soft and Spontaneous CP Violation.

Paul H. Frampton and Masayasu Harada

Department of Physics and Astronomy,

University of North Carolina, Chapel Hill, NC 27599-3255

Abstract

We study four different models for CP violation: the standard (KM) model, the aspon model of spontaneous breaking and two models of soft breaking. In all except the standard model, the strong CP problem is addressed and solved. Testable predictions for the area of the unitarity triangle and for $(\epsilon'/\epsilon)_K$ are emphasized. The issue of CP violation may well become the first place where the standard model of particle theory is shown definitively to be deficient. There are two reasons for expecting this to happen: (1) the strong CP problem is still not understood in the unadorned standard model and (2) the KM mechanism, although unquestionably present, may not provide the full explanation of ϵ_K and $(\epsilon'/\epsilon)_K$.

I. INTRODUCTION

There are several models for describing CP violation by scalar dynamics. Spontaneous CP violation [1,2] is one of the interesting schemes, especially where CP is broken simultaneously with $SU(2)_L \times U(1)_Y$. This kind of models has been widely studied (see *e.g.* Refs. [3–5]).

There are other models in which heavy quarks and scalars are introduced and CP violation is originated in the heavy scalar sector. The CP violation is transported to the ordinary quark sector through the Yukawa interactions among heavy quark, ordinary quark and heavy scalar. At the same time, an attempt is made to resolve the Strong CP problem. These models may be divided into two classes by the existence of the tree level flavor changing neutral current (FCNC).

There are two typical models without tree level FCNC. In one class of models only right-handed quarks have Yukawa interactions with heavy quarks and scalars [6], while in another class only left-handed quarks have the Yukawa interaction [7]. In both models CP is violated in the heavy mass terms softly or spontaneously.

A typical model with the tree level FCNC is the Aspon model [8]. This model is widely studied (see, *e.g.* Refs. [9,10]). In this model one vector-like $SU(2)_L$ doublet of quarks are introduced. Those quarks have same charges as up- and down-types of ordinary quarks. Two heavy $SU(2)_L \times U(1)_Y$ singlet scalars have VEVs which break CP spontaneously. Another model with tree level FCNC is given in [11], where unlike the models considered here, no additional $U(1)$ symmetry occurs.

In this paper we study constraints and predictions of the above two models of soft CP breaking comparing with those for the Aspon model. These considerations are timely because experiments are underway to measure both $\text{Re}(\epsilon'/\epsilon)$ and the CP asymmetries in B^0 decays. In fact, there are two experiments each to measure both effects. The former is being measured by the NA-48 experiment at CERN, and by the E799/E832 (KTEV) experiment at FermiLab. The latter is being studied by the BaBar detector of the PEP-II experiment at SLAC and by the BELLE experiment at the KEK B-Factory.

The layout of the paper is as follows: In Section(II) we describe in detail the different models we shall analyze. In Section(III) the constraints arising from ϵ_K are derived. The predictions for ϵ'/ϵ are given in Section(IV). In Section(V) the constraint of $B - \bar{B}$ mixing is discussed. Section(VI) covers the CP asymmetry predictions for neutral B decay. In Section(VII) the lower limits on $\bar{\Theta}$ are calculated, together with the corresponding lower limits on the neutron electric dipole moment. Finally in Section(VIII) the different predictions are summarized.

II. MODELS

Here we shall list four different models for CP violation which exemplify all of the ideas we are considering. At the end of the paper we shall summarize the similarities and differences of the experimental predictions. Thus the hurried reader could read just this section and that summary to sample the main points: the intervening sections provide technical details.

A. Standard Model

The first model is just the standard model (SM) with the KM mechanism [12] of explicit CP violation. Principally, we are interested in models which also solve strong CP (as all the other three will). The standard model requires an additional mechanism (*e.g.* the Peccei-Quinn mechanism [13] or massless up quark (see, *e.g.* Ref. [14]) to accomplish this. Nevertheless, it forms an essential comparison for all the other cases.

B. Two Models (Types L and R) of Soft CP Breaking

The class of models we consider for soft CP violation is constructed by adding two $SU(2)_L$ singlet scalars χ_I ($I = 1, 2$) with hyper-charge Y_χ and one non-chiral quark Q to the standard model (SM). These Q and χ_I carry the opposite charges of an extra $U(1)_{\text{new}}$ symmetry. The hypercharge of Q is determined in such a way that the Yukawa interactions

among χ_I , Q and the ordinary quark q are allowed: $Y_Q = Y_\chi + Y_q$. The Yukawa interactions in the models can be written as

$$\mathcal{L}_Y = - \sum_{I=1}^2 \sum_{i=1}^3 h_i^I \left[\overline{Q} q_i \chi_I + \overline{q}_i Q \chi_I^* \right] , \quad (2.1)$$

where h_i^I is a real Yukawa coupling.

CP is softly broken by the mass term of χ_I . The models in this category are divided into two types by the chirality of the ordinary quark q which couples to Q and χ_I : in the first type (Type R), q is a right-handed down-type quark, $Y_q = -1/3$ [6]; in the second type (Type L), q is a left-handed $SU(2)_L$ doublet quark, $Y_q = 1/6$ [7].

Let us explain details of these models for soft CP violation. The scalar potential for χ_I is given by

$$\mathcal{L}_\chi = \sum_{I,J,K,L=1}^2 \overline{\lambda}_{IJKL} \chi_I^* \chi_J \chi_K^* \chi_L + \sum_{I,J=1}^2 \overline{M}_{IJ} \chi_I^* \chi_J , \quad (2.2)$$

where $\overline{\lambda}_{IJKL}$ and $\overline{M}_{II} = \overline{M}_{II}^*$ are real quantities and $\overline{M}_{12} = \overline{M}_{21}^*$ is a complex quantity. The interaction between χ_I and the ordinary $SU(2)_L$ doublet Higgs scalar H is given by

$$\mathcal{L}_{\chi H} = \left(H^\dagger H - \frac{v^2}{2} \right) \sum_{I,J=1}^2 \lambda_{IJ} \chi_I^* \chi_J , \quad (2.3)$$

where λ_{IJ} is real. The mass eigenstate χ'_I is given by a unitary rotation:

$$\chi'_I = \sum_{J=1}^2 U_{IJ} \chi_J , \quad (2.4)$$

where U is a suitable unitary matrix.

After rotating χ to the mass eigenstate χ' as in Eq. (2.4), the Yukawa interactions become

$$\mathcal{L}_Y = - \sum_{I=1}^2 \sum_{i=1}^3 \left[f_{Ii} \overline{Q} q_i \chi'_I + f_{Ii}^* \overline{q}_i Q \chi'^*_I \right] , \quad (2.5)$$

where $f_{Ii} = \sum_{J=1}^2 U_{IJ}^* h_i^J$ is a complex Yukawa coupling.

An important combination for CP measurement is $X_{ij}^I \equiv f_{Ii}^* f_{Ij}$. The fact that the original Yukawa coupling h_i^I is real leads

$$\text{Im} \left(X_{ij}^{I=2} \right) = -\text{Im} \left(X_{ij}^{I=1} \right) . \quad (2.6)$$

C. Aspon Model

Here the complex scalar χ_I has a Vacuum Expectation Value (VEV) which spontaneously breaks CP (Aspon model [8]); In the Aspon model the $U(1)_{\text{new}}$ is gauged, and the gauge boson acquires its mass from the VEV of χ_I . Q and q have same charges ($Y_\chi = 0$, $Y_Q = Y_q$), and they have complex mass mixing. Accordingly, there exist tree-level flavor changing neutral currents (FCNC) mediated by the Aspon gauge boson and χ_I .

Let us briefly review the relevant part of the Aspon model. In the Aspon model q can be the left-handed doublet quarks, or the right-handed down-type quarks, in the simplest versions. In the present analysis we fix q to be the left-handed doublet quarks for definiteness.¹ All the couplings in the scalar potentials in Eqs. (2.2) and (2.3) are real, and CP is spontaneously broken by the VEV of χ_I :

$$\langle \chi_1 \rangle = \frac{1}{\sqrt{2}} \kappa_1 e^{i\theta} , \quad \langle \chi_2 \rangle = \frac{1}{\sqrt{2}} \kappa_2 . \quad (2.7)$$

As a result the light quarks q mix with the non-chiral heavy quark Q . The mass matrix, in the weak basis where 3×3 submatrix for down sector is diagonal, is given by [9]

$$\mathcal{M}_d = \begin{pmatrix} m_d & 0 & 0 & F_1 \\ 0 & m_s & 0 & F_2 \\ 0 & 0 & m_b & F_3 \\ 0 & 0 & 0 & M_Q \end{pmatrix} , \quad (2.8)$$

where

$$F_i = h_i^1 \langle \chi_1 \rangle + h_i^2 \langle \chi_2 \rangle . \quad (2.9)$$

This mass matrix is diagonalized by a biunitary transformation, $K_L^\dagger \mathcal{M}_d K_R$. The approximate form of the transformation matrices are given by [9]

¹In the concluding section VIII we mention the difference in predictions for an R-type Aspon model.

$$\begin{aligned}
K_L &= \begin{pmatrix} 1 - \frac{1}{2} |x_1|^2 & x_1 x_2^* \frac{m_s^2}{m_d^2 - m_s^2} & x_1 x_3^* \frac{m_b^2}{m_d^2 - m_b^2} & x_1 \\ x_2 x_1^* \frac{m_d^2}{m_s^2 - m_d^2} & 1 - \frac{1}{2} |x_2|^2 & x_2 x_3^* \frac{m_b^2}{m_s^2 - m_b^2} & x_2 \\ x_3 x_1^* \frac{m_d^2}{m_b^2 - m_d^2} & x_3 x_2^* \frac{m_s^2}{m_b^2 - m_s^2} & 1 - \frac{1}{2} |x_3|^2 & x_3 \\ -x_1^* & -x_2^* & -x_3^* & 1 - \frac{1}{2} \sum_{j=1}^3 |x_j|^2 \end{pmatrix}, \\
K_R &= \begin{pmatrix} 1 & x_1 x_2^* \frac{m_d m_s}{m_d^2 - m_s^2} & x_1 x_3^* \frac{m_d m_b}{m_d^2 - m_b^2} & \frac{m_d}{M_Q} x_1 \\ x_2 x_1^* \frac{m_s m_d}{m_s^2 - m_d^2} & 1 & x_2 x_3^* \frac{m_s m_b}{m_s^2 - m_b^2} & \frac{m_s}{M_Q} x_2 \\ x_3 x_1^* \frac{m_b m_d}{m_b^2 - m_d^2} & x_3 x_2^* \frac{m_b m_s}{m_b^2 - m_s^2} & 1 & \frac{m_b}{M_Q} x_3 \\ -\frac{m_d}{M_Q} x_1^* & -\frac{m_s}{M_Q} x_2^* & -\frac{m_b}{M_Q} x_3^* & 1 \end{pmatrix}, \tag{2.10}
\end{aligned}$$

where

$$x_i \equiv F_i/M_Q. \tag{2.11}$$

In the weak basis the Aspon gauge boson does not couple to light quarks. However, due to the mixing with the heavy quark Q , light quarks in terms of the mass eigenstates couple to the Aspon gauge boson. This induces FCNC's:

$$\mathcal{L}_A^{\text{FCNC}}(\text{down}) = -g_A \alpha_{ij} \bar{d}_L^i \gamma_\mu d_L^j A^\mu, \tag{2.12}$$

where

$$\begin{aligned}
\alpha_{ij} &\simeq x_i x_j^*, \quad (i, j = 1, 2, 3), \\
\alpha_{4i} &= \alpha_{i4}^* \simeq -x_i^*, \quad (i = 1, 2, 3), \\
\alpha_{44} &\simeq 1 - \sum_{i=1}^3 |x_i|^2, \tag{2.13}
\end{aligned}$$

with A^μ being the Aspon gauge boson and g_A the gauge coupling. In addition to the above FCNC's in the left-handed sector there exist FCNC's in the right-handed sector. However, the coupling is suppressed by the mass ratio m_i/M_Q , where $m_i = (m_d, m_s, m_b)$. Similarly, flavor changing couplings to χ_I are suppressed by m_i/M_Q . So we will neglect these couplings below.

III. CONSTRAINT FROM ϵ_K

In the SM, ϵ_K arises from the W^+W^- exchange box diagram, and is proportional to a combination of CKM angles and to $\sin \delta$ where δ is the KM phase, and therefore gives a constraint between these SM parameters.

Now we study the other models defined in Section(II). The parameter ϵ_K is given by

$$\epsilon_K = \frac{e^{i\pi/4}}{2\sqrt{2}} \left[\frac{\text{Im}M_{12}}{\text{Re}M_{12}} + 2\frac{\text{Im}A_0}{\text{Re}A_0} \right]. \quad (3.1)$$

The second term is related to ϵ'/ϵ , and much smaller than the first term as we shall see below.

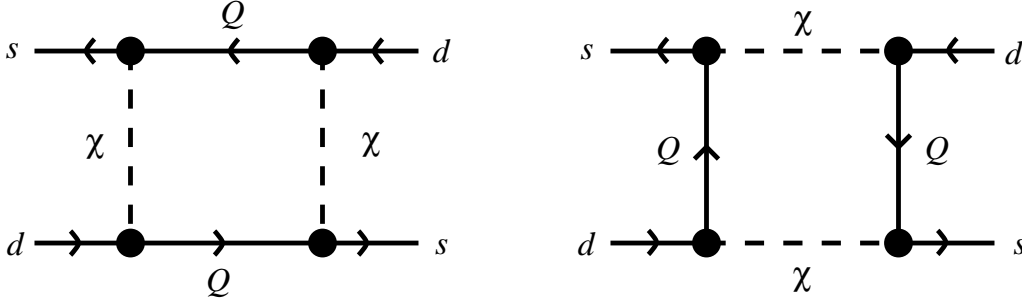


FIG. 1. Box diagram contributions to $K^0-\bar{K}^0$ mixing in the models of soft CP breaking.

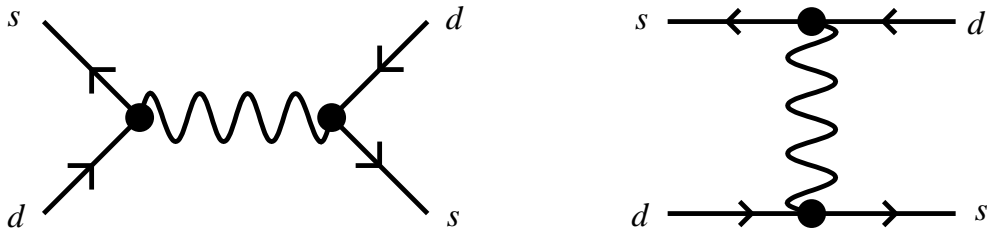


FIG. 2. Tree level Aspon gauge boson exchange contributions to $K^0-\bar{K}^0$ mixing in the Aspon model.

The dominant contribution to $\text{Im}M_{12}$ is given by the scalar-heavy quark exchange box diagram shown in Fig. 1 for the models of soft CP breaking, and by the Aspon gauge boson exchange tree diagram shown in Fig. 2 for the Aspon model. The effective $\Delta S = 2$ Hamiltonian derived from the contribution, for Type R soft breaking, is given by

$$\mathcal{H}_{\Delta S=2}^{(\text{new})} = \frac{1}{v^2} C_{sd}^{(R)} (\bar{s}_R \gamma^\mu d_R) (\bar{s}_R \gamma_\mu d_R) , \quad (3.2)$$

where

$$C_{sd}^{(R)} = \frac{1}{6(4\pi)^2} \frac{v^2}{M_Q^2} \sum_{I,J=1}^2 X_{sd}^I X_{sd}^J F(r_I, r_J) , \quad (3.3)$$

with $r_I = M_I^2/M_Q^2$. The function $F(r_I, r_J)$ is defined by

$$F(r_I, r_J) = \frac{3}{(1-r_I)(1-r_J)} - \frac{3r_J^2}{(1-r_J)^2(r_I-r_J)} \ln r_J + \frac{3r_I^2}{(1-r_I)^2(r_I-r_J)} \ln r_I , \quad (3.4)$$

where the normalization of $F(r_I, r_J)$ is taken as $F(1, 1) = 1$. For Type L soft breaking, and for the Aspon model, the effective coupling is the same as Eq. (3.2) with the helicities switched from R to L, and with the coefficient $C_{sd}^{(R)}$ replaced by $C_{sd}^{(L)}$, and $C_{sd}^{(A)}$, respectively. The formula for $C_{sd}^{(L)}$ is exactly as for $C_{sd}^{(R)}$ in Eq.(3.3). We will give the formula for $C_{sd}^{(A)}$ later.

As in the SM, $\text{Re}M_{12}$ is dominated by the contribution from W -charm exchange box diagram. This is given by

$$\mathcal{H}_{\Delta S=2}^{(\text{KM})} = \frac{1}{v^2} C_{sd}^{(\text{KM})} (\bar{s}_L \gamma^\mu d_L) (\bar{s}_L \gamma_\mu d_L) , \quad (3.5)$$

where

$$C_{sd}^{(\text{KM})} = \frac{1}{8\pi^2} \frac{M_W^2}{v^2} (V_{cs}^* V_{cd})^2 S\left(\frac{m_c^2}{M_W^2}\right) . \quad (3.6)$$

The function $S(x)$ is so-called Inami-Lim function [15] and $S(m_c^2/M_W^2) \simeq 3.48 \times 10^{-4}$. V_{cs} and V_{cd} are corresponding elements of the quark mixing matrix, $|V_{cs}^* V_{cd}| \simeq 0.22$. Note that the mixing matrix for the models of soft CP breaking is real and orthogonal, and the 3×3 submatrix of it in the Aspon model is also real and orthogonal to a very good approximation [16].

Since QCD respects parity invariance, it may be enough to assume that two operators in Eqs. (3.2) and (3.5) give the same hadron matrix elements. Then $|\epsilon_K|$ can be expressed as

$$|\epsilon_K| \simeq \frac{1}{2\sqrt{2}} \left| \frac{\text{Im} C_{sd}^{(R,L,A)}}{C_{sd}^{(\text{KM})}} \right|. \quad (3.7)$$

The experimental value $|\epsilon_K| = 2.26 \times 10^{-3}$ gives a constraint to $|\text{Im} C_{sd}|$:

$$|\text{Im} C_{sd}^{(R,L,A)}| \simeq 1.4 \times 10^{-10}. \quad (3.8)$$

This smallness of $|\text{Im} C_{sd}^{(R,L,A)}|$ is easily understood by small Yukawa coupling f_{Ii} .

To estimate the size of the Yukawa couplings, we can assume that their real and imaginary parts are comparable, equate M_Q and M_I and arrive, from Eq.(3.3), at:

$$\frac{v}{M_Q} \bar{X}_{sd}^{(R,L)} \simeq 3 \times 10^{-4}, \quad (3.9)$$

where we have defined $(\bar{X}_{sd})^2 = \frac{1}{2} |\text{Im} X_{sd}^{I=1} \sum_{I=1}^2 \text{Re} X_{sd}^I|$ using the fact that $\text{Im} X_{sd}^{I=2} = -\text{Im} X_{sd}^{I=1}$. Of course, the corresponding Yukawa couplings involving the third family, *e.g.* \bar{X}_{bd} , \bar{X}_{bs} are not constrained by ϵ_K . It seems natural to say that M_Q is bigger than the weak scale, and then Eq. (3.9) gives the lower bound $\bar{X}_{sd}^{(R,L)} \gtrsim 3 \times 10^{-4}$.

In the Aspon model

$$C_{ds}^{(A)} = 2 \left(\frac{v}{\kappa} \right)^2 (x_1^* x_2)^2 \quad (3.10)$$

where κ is the scale of $U(1)_{\text{new}}$ breaking. The combination of Eq. (3.8) and Eq. (3.10), as is well-known [9,17], gives a constraint on κ , using information from $\bar{\Theta}$ (see Section(VII)). The parameter x_3 is not constrained by ϵ_K .

IV. PREDICTIONS FOR REAL PART OF (ϵ'/ϵ)

In the standard model, an enormous effort has gone into calculating direct CP violation, characterized by the quantity $\text{Re}(\epsilon'/\epsilon)$ (see, *e.g.* Refs. [18–21]). There remains some uncertainties in the prediction due to the quark masses, especially m_s , the QCD scale Λ_{QCD} , and certain hadronic matrix elements. One quoted range is [19]:

$$\text{Re} \left(\frac{\epsilon'}{\epsilon} \right) = (3.6 \pm 3.4) \times 10^{-4} \quad (4.1)$$

In particular, a vanishing result results from an accidental cancellation (rather than a symmetry).

The parameter ϵ' is given by

$$\epsilon' = -\frac{e^{i(\pi/2+\delta_2-\delta_0)}}{\sqrt{2}} \frac{\text{Re}A_2}{\text{Re}A_0} \left[\frac{\text{Im}A_0}{\text{Re}A_0} - \frac{\text{Im}A_2}{\text{Re}A_2} \right] , \quad (4.2)$$

where A_I are the isospin amplitudes in $K \rightarrow \pi\pi$ decays and δ_I are the corresponding final state interaction phases.

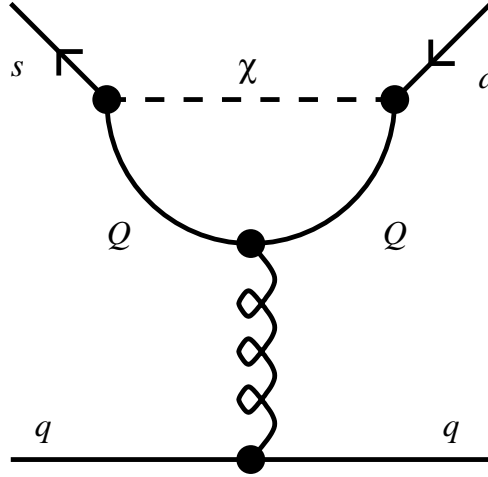


FIG. 3. Gluon penguin diagram contribution to the imaginary part of the $K \rightarrow \pi\pi$ decay for the models of soft CP breaking.

To estimate the contributions to the imaginary part of the $K \rightarrow \pi\pi$ decay for the models of soft CP breaking, let us consider the gluon penguin diagram shown in Fig. 3. For Type R soft CP breaking model the chiralities of s and d quarks in the external lines are different with those for the W -exchange contribution. Then it is convenient to define the following operators:

$$\begin{aligned} Q'_3 &= 4 (\bar{s}_R \gamma_\mu d_R) \sum_{q=u,d,s} (\bar{q}_R \gamma^\mu q_R) , \\ Q'_4 &= 4 \sum_{q=u,d,s} (\bar{s}_R \gamma_\mu q_R) (\bar{q}_R \gamma^\mu d_R) , \\ Q'_5 &= 4 (\bar{s}_R \gamma_\mu d_R) \sum_{q=u,d,s} (\bar{q}_L \gamma^\mu q_L) , \\ Q'_6 &= -8 \sum_{q=u,d,s} (\bar{s}_R q_L) (\bar{q}_L d_R) . \end{aligned} \quad (4.3)$$

By using these operators, the $\Delta S = 1$ effective Hamiltonian for Type R soft CP breaking model is given by

$$\mathcal{H}_{\Delta S=1}^{(\text{new})} = \frac{1}{v^2} \overline{C}_{sd}^{(R)} \sum_{i=3}^6 \nu_i(M_{\text{new}}) Q'_i(M_{\text{new}}) , \quad (4.4)$$

where M_{new} is a scale around masses of new particles, and

$$-\frac{1}{3}\nu_3(M_{\text{new}}) = \nu_4(M_{\text{new}}) = -\frac{1}{3}\nu_5(M_{\text{new}}) = \nu_6(M_{\text{new}}) = \frac{\alpha_s(M_{\text{new}})}{256\pi} . \quad (4.5)$$

Here $\overline{C}_{sd}^{(R)}$ is expressed as

$$\overline{C}_{sd}^{(R)} = \frac{v^2}{M_Q^2} \sum_{I=1}^2 X_{sd}^I \tilde{F} \left(\frac{M_I^2}{M_Q^2} \right) , \quad (4.6)$$

where

$$\tilde{F}(r_I) = \frac{4}{3(1-r_I)} \left[\frac{7-29r_I+16r_I^2}{6(1-r_I)^2} - \frac{r_I(3-2r_I)}{(1-r_I)^3} \ln r_I \right] . \quad (4.7)$$

The effective Hamiltonian for the Type L soft CP breaking is obtained by switching the helicities R to L and L to R in the above expressions, and $\overline{C}_{sd}^{(L)} = \overline{C}_{sd}^{(R)}$.

To obtain the amplitudes for $K \rightarrow \pi\pi$ we need to study the renormalization group evolution of the coefficients. This is done by using the method described in, *e.g.* Refs. [20,21]. The resultant coefficients are $(\nu_3(m_c), \nu_4(m_c), \nu_5(m_c), \nu_6(m_c)) = (-1.2, 1.5, 0.8, 4.7) \times 10^{-4}$, where we have taken $M_{\text{new}} = M_W$ for simplicity. As is well known, the gluon penguin diagram gives a contribution to only isospin zero channel. We use the values in Ref. [21] for the hadron matrix elements: $(\langle Q'_3(m_c) \rangle_0, \langle Q'_4(m_c) \rangle_0, \langle Q'_5(m_c) \rangle_0, \langle Q'_6(m_c) \rangle_0) = (-0.01, -0.19, 0.09, 0.28) (\text{GeV})^3$. By using the experimental values $\text{Re}A_0 = 3.33 \times 10^{-7} \text{ GeV}$ and $\text{Re}A_2 = 1.50 \times 10^{-8} \text{ GeV}$ with $|\epsilon_K| = 2.36 \times 10^{-3}$, $\text{Re}(\epsilon'/\epsilon)$ from the gluon-penguin diagram is given by

$$\left| \text{Re} \left(\frac{\epsilon'}{\epsilon} \right) \right| \simeq (7.7 \times 10^{-2}) \left| \text{Im} \overline{C}_{sd}^{(R,L)} \right| . \quad (4.8)$$

Assuming that the real and imaginary parts of the Yukawa coupling are comparable, and using the value in Eq. (3.9) estimated from ϵ_K , we obtain

$$\left| \text{Re} \left(\frac{\epsilon'}{\epsilon} \right) \right| \simeq 2 \times 10^{-5} \frac{v}{M_Q} \lesssim 2 \times 10^{-5} \quad (4.9)$$

for the models of soft CP breaking. Note that $\text{Re}(\epsilon'/\epsilon)$ can be of order 10^{-4} if we allow that the imaginary part is bigger than the real part of X_{sd}^I , $\text{Im}X_{sd}^I \sim 10 \times \text{Re}X_{sd}^I$. The prediction in Eq.(4.8) is more reliable than the corresponding prediction in the standard model because there is no expectation of delicate cancellation between diagrams.

In the Aspon model the dominant contribution is given by the Aspon gauge boson-heavy quark exchange penguin diagram, and $\text{Re}(\epsilon'/\epsilon)$ is estimated as [22] $\text{Re}(\epsilon'/\epsilon) \lesssim 10^{-5}$.

V. $B^0 - \bar{B}^0$ MIXING

In addition to the W -exchange box diagram contribution the scalar-heavy quark exchange box diagram contribute to $B_d - \bar{B}_d$ mixing in the models of soft CP violation. The effective Hamiltonian derived from the new contribution for the Type R soft CP breaking model takes the same form as that for $\Delta S = 1$ effective Hamiltonian given in Eq. (3.2) with s replaced by b , and similarly for the Type L soft CP breaking model and the Aspon model. This should be compared with the W -top exchange diagram contribution, which takes the same form as that in Eq. (3.5) with s and c replaced by b and t . Again it may be enough to assume that the two operators with different chiralities give the same hadron matrix elements. Then let us compare C_{bd} with $C_{bd}^{(\text{KM})}$.

The experimental value of the top quark mass, $m_t = 175 \text{ GeV}$, gives $C_{bd}^{(\text{KM})} \simeq (3.46 \times 10^{-3}) (V_{tb}V_{td})$. In the models of soft CP breaking the quark mixing matrix is real and orthogonal, and the unitarity triangle is flat. In the Aspon model the imaginary parts of the mixing matrix arise from the imaginary parts of the small quantities x_i , and the 3×3 submatrix is real and orthogonal in good approximation. So the current experimental value $|(V_{ud}^*V_{ub}) / (V_{cd}^*V_{cb})| \simeq 0.35$ leads $|(V_{td}^*V_{tb}) / (V_{cd}^*V_{cb})| \simeq 0.65$, and $|V_{td}^*V_{tb}| \simeq 5.9 \times 10^{-3}$. This implies $C_{bd}^{(\text{KM})} \simeq 1.2 \times 10^{-7}$. On the other hand, when we assume that the Yukawa couplings are independent of the generation in the models for soft or spontaneous CP violation con-

sidered in this paper, C_{bd} is roughly of the same order as C_{sd} ; $|C_{bd}^{(R,L,A)}| \sim |C_{sd}^{(R,L,A)}| \sim 10^{-10}$. This value is much smaller than $C_{bd}^{(\text{KM})}$, and negligible. This situation is similar to $\eta = 0$ in the standard model, which is not excluded by the experiment [16,23,24].

In the case of generation-*independent* Yukawa couplings, CP violation in $B_d-\bar{B}_d$ mixing is much smaller for the soft and spontaneous CP breaking models than that for the SM. On the other hand, we can admit generation-*dependent* Yukawa couplings, and expect that C_{bd} is larger and roughly of the same order as $C_{bd}^{(\text{KM})}$; $|C_{bd}^{(R,L,A)}| \simeq 10^{-7}$. For the models of soft CP breaking this corresponds to:

$$\frac{v}{M_Q} |X_{bd}| \simeq 7 \times 10^{-3} , \quad (5.1)$$

where X_{bd} is the average value of $X_{bd}^{I=1}$ and $X_{bd}^{I=2}$. [Note that $\text{Im}X_{bd} = \text{Im}X_{bd}^{I=1} = -\text{Im}X_{bd}^{I=2}$.] For the Aspon model $|C_{bd}^{(A)}| \simeq 10^{-7}$ leads

$$\frac{v}{\kappa} |x_1^* x_3| \simeq 2 \times 10^{-4} . \quad (5.2)$$

For the Type R soft breaking model $\text{Im}X_{bd}$ is strongly constrained by $\bar{\Theta}$, $|\text{Im}X_{bd}| \lesssim 2 \times 10^{-4}$ (see Eq. (7.6)). So the above constraint (5.1) for $|X_{bd}|$ leads that $|\text{Re}X_{bd}|$ is much bigger than $|\text{Im}X_{bd}|$. This implies that the CP violation in $B_d-\bar{B}_d$ mixing in the Type R soft breaking model is much smaller than that in the SM even if we introduce the generation-dependent Yukawa coupling. For the Type L soft breaking model and the Aspon model, however, the constraint from $\bar{\Theta}$ is not strong, so that the CP violation in the $B_d-\bar{B}_d$ mixing can be as big as in the SM.

Similarly, for $B_s-\bar{B}_s$ mixing, we may expect that C_{bs} is as large as $C_{bs}^{(\text{KM})}$. In such a case, the CP violation in the $B_s-\bar{B}_s$ mixing for the Type L soft breaking model and the Aspon model can be as large as in the SM. On the other hand, due to the constraint from $\bar{\Theta}$, for the Type R soft breaking model it is much smaller than that in the SM.

VI. NEUTRAL B DECAYS AND CP ASYMMETRIES.

The CP violation in the neutral B meson decays is expressed by the product of the two quantities measuring the indirect and direct CP violations, respectively:

$$\lambda(B_q \rightarrow X) = \left(\frac{q}{p}\right)_{B_q} \frac{\bar{A}(\bar{B}_q \rightarrow \bar{X})}{A(B_q \rightarrow X)}, \quad (6.1)$$

where B_q is B_d or B_s . In the SM this quantity measures the angles of the unitarity triangle. This corresponds to the terms in the requirement that:

$$V_{ub}^* V_{ud} + V_{cb}^* V_{cd} + V_{tb}^* V_{td} = 0. \quad (6.2)$$

The angles between the 1st & 2nd, 2nd & 3rd, and 3rd & 1st terms are called γ , α , and β respectively. The KM model predicts a sizeable area of the triangle involving, *e.g.* $\sin 2\beta > 0.65$ [24].

To study the quantity λ in Eq. (6.1) in the soft and spontaneously broken models, let us consider four cases for the coefficients of the 4-fermi operator as in Eqs. (3.2) and (3.5). (An alternative analysis of new physics and the quantity λ is in [25].)

The first case corresponds to generation-independent Yukawa couplings. The other three cases involve generation dependence, in particular where the third generation couples more strongly than the second (case 2), the first (case 3) or both (case 4); these lead, in general, to a deviation from pure superweak phenomenology. The four cases are explicitly:

1. $|\text{Im}C_{bd}| \sim |\text{Im}C_{bs}| \sim |\text{Im}C_{sd}|$;
2. $|\text{Im}C_{bs}| \sim |\text{Im}C_{sd}|$ and $|\text{Im}C_{bd}| \sim |C_{bd}^{(\text{KM})}|$;
3. $|\text{Im}C_{bd}| \sim |\text{Im}C_{sd}|$ and $|\text{Im}C_{bs}| \sim |C_{bs}^{(\text{KM})}|$;
4. $|\text{Im}C_{bd}| \sim |C_{bd}^{(\text{KM})}|$ and $|\text{Im}C_{bs}| \sim |C_{bs}^{(\text{KM})}|$;

The first factor $(q/p)_{B_q}$ in Eq. (6.1) measures the indirect CP violation. In the present models, up to corrections of order 10^{-2} , it is given by the quantity with modulus one,

$$\left(\frac{q}{p}\right)_{B_q} \simeq \frac{C_{bq}^{(\text{KM})} + C_{bq}}{|C_{bq}^{(\text{KM})} + C_{bq}|}. \quad (6.3)$$

Then for $\text{Im}C_{bq} \sim \text{Im}C_{sd}$ we find $\text{Im}(q/p)_{B_q} \lesssim 10^{-2}$. Note that any non-vanishing value for $\text{Im}(q/p)_{B_q}$ comes from the approximation involved in Eq. (6.3). On the other hand, for $|\text{Im}C_{bq}| \sim |C_{bq}^{(\text{KM})}|$ as in 2, 3 and 4 (as in the SM), which is possible for the Aspon model and the Type L soft breaking model, the $\text{Im}C_{bq}$ becomes less negligible and so it is convenient to define

$$\left(\frac{q}{p}\right)_{B_q} \simeq e^{i2\tilde{\beta}_q}. \quad (6.4)$$

The second factor (\bar{A}/A) in Eq. (6.1) measures direct CP violation in neutral B meson decays. Neutral B meson decays are described by $\bar{b} \rightarrow q'\bar{q}q''$ at the quark level. In this case the ratio of W -exchange penguin contribution to the tree contribution is roughly [26]

$$\frac{A_{\text{penguin}}^{(\text{KM})}}{A_{\text{tree}}} \sim (4\text{-}10\%) \frac{V_{tb}^* V_{tq''}}{V_{q'b}^* V_{q'q''}}. \quad (6.5)$$

In addition, there is a contribution from the scalar-heavy quark exchange penguin diagram in the soft breaking models, and a contribution from the Aspon gauge boson-heavy quark exchange penguin diagram in the Aspon model. The ratio of the new penguin contribution to the W -top penguin contribution is given by

$$\frac{A_{\text{penguin}}^{(\text{new})}}{A_{\text{penguin}}^{(\text{KM})}} \sim \frac{\bar{C}_{bq''}}{\bar{C}_{bq''}^{(\text{KM})}}, \quad (6.6)$$

where $\bar{C}_{bq''}$ and $\bar{C}_{bq''}^{(\text{KM})}$ are analogues of \bar{C}_{sd} in Eq. (4.4). This ratio is estimated by the ratio of the couplings:

$$\frac{\bar{C}_{bq''}}{\bar{C}_{bq''}^{(\text{KM})}} \sim \begin{cases} \left(\frac{v}{M_Q}\right)^2 \frac{X_{bq''}}{V_{tb}^* V_{tq''}}, & \text{for the soft breaking models,} \\ \left(\frac{v}{\kappa}\right)^2 \frac{x_3 x_{q''}^*}{V_{tb}^* V_{tq''}}, & \text{for the Aspon model,} \end{cases} \quad (6.7)$$

where $x_{d,s} = x_{1,2}$. For $\text{Im}C_{bq''} \sim \text{Im}C_{sd}$, the imaginary part of this ratio is very small, and the new contribution is negligible compared with the KM-penguin contribution. When

$|\text{Im}C_{bq''}| \sim |C_{bq''}^{(\text{KM})}|$, the imaginary part of this ratio can be of order one in the Type L soft breaking model, while it is small, $\lesssim 10^{-1}$, in the Aspon model. Then if

$$\left| \frac{V_{tb}V_{tq''}}{V_{q'b}V_{q'q''}} \right| \leq 1, \quad (6.8)$$

the tree diagram dominates over penguin diagram [26], and the direct CP violation in the B system is small. This corresponds to the processes $b \rightarrow c\bar{c}s$, $b \rightarrow c\bar{c}d$ and $b \rightarrow u\bar{u}d$. On the other hand, if tree diagrams are forbidden, the penguin diagram dominates, and

$$\frac{\bar{A}}{A} \sim \frac{\overline{C}_{bq''}^{(\text{KM})} + \overline{C}_{bq''}^*}{\overline{C}_{bq''}^{(\text{KM})} + \overline{C}_{bq''}}. \quad (6.9)$$

This is for $q' = d$ or s . When $|\text{Im}C_{bq''}| \sim |C_{bq''}^{(\text{KM})}|$ in this case, it is convenient to parameterize

$$\frac{\bar{A}}{A} \simeq e^{i2\tilde{\alpha}_{q''}}, \quad (6.10)$$

where $\tilde{\alpha}_{q''}$ is of order one in the Type L soft breaking model, $\lesssim 10^{-1}$ in the Aspon model, and very small in the Type R soft breaking model.

In Table I we show examples of neutral B meson decay modes with values of $\text{Im}\lambda(B_q \rightarrow X)$ for the four cases discussed above. One can read from Table I specific features of the present models. For example: if CP asymmetry in $B_d \rightarrow K_S K_S$ were large, then it indicates a clear deviation from the Standard Model, and those for tree dominant decay modes are the same; $\text{Im}\lambda(B_d \rightarrow \psi K_S) \simeq \text{Im}\lambda(B_d \rightarrow D^+ D^-) \simeq \text{Im}\lambda(B_d \rightarrow \pi^+ \pi^-)$. On the other hand, if it were small, all CP violations in B_d decays are small.

If we focus just on the “gold-plated” decay mode $B \rightarrow \psi K_S$ (top row of Table I) - where the SM predicts an unmistakable large CP asymmetry - then in the Type R soft breaking model one must have condition (1) and hence a very small β ($\beta < 10^{-2}$); in the Type L soft breaking model or the Aspon model one *can* admit conditions (2) and (4) and hence large effective β . However, if we impose that the Yukawa couplings are generation-independent, all except the SM predict a CP asymmetry in this mode too small to be detected.

		(1)	(2)	(3)	(4)	SM
$b \rightarrow c\bar{c}s$	$B_d \rightarrow \psi K_S$	0	$\sin 2\tilde{\beta}_d$	0	$\sin 2\tilde{\beta}_d$	$-\sin 2\beta$
	$B_s \rightarrow D_s^+ D_s^-$	0	0	$\sin 2\tilde{\beta}_s$	$\sin 2\tilde{\beta}_s$	$-\sin 2\beta'$
$b \rightarrow c\bar{c}d$	$B_d \rightarrow D^+ D^-$	0	$\sin 2\tilde{\beta}_d$	0	$\sin 2\tilde{\beta}_d$	$-\sin 2\beta$
	$B_s \rightarrow \psi K_S$	0	0	$\sin 2\tilde{\beta}_s$	$\sin 2\tilde{\beta}_s$	$-\sin 2\beta'$
$b \rightarrow c\bar{c}s$	$B_d \rightarrow \pi^+ \pi^-$	0	$\sin 2\tilde{\beta}_d$	0	$\sin 2\tilde{\beta}_d$	$\sin 2\alpha$
	$B_s \rightarrow \rho K_S$	0	0	$\sin 2\tilde{\beta}_s$	$\sin 2\tilde{\beta}_s$	$-\sin 2(\gamma + \beta')$
$b \rightarrow s\bar{s}s$	$B_d \rightarrow \phi K_S$	0	$\sin 2\tilde{\beta}_d$	$\sin 2\tilde{\alpha}_s$	$\sin 2(\tilde{\beta}_d + \tilde{\alpha}_s)$	$-\sin 2(\beta - \beta')$
	$B_s \rightarrow \eta' \eta'$	0	0	$\sin 2(\tilde{\beta}_s + \tilde{\alpha}_s)$	$\sin 2(\tilde{\beta}_s + \tilde{\alpha}_s)$	0
$b \rightarrow s\bar{s}d$	$B_d \rightarrow K_S K_S$	0	$\sin 2(\tilde{\beta}_d + \tilde{\alpha}_d)$	0	$\sin 2(\tilde{\beta}_d + \tilde{\alpha}_d)$	0
	$B_s \rightarrow \phi K_S$	0	$\sin 2\tilde{\alpha}_d$	$\sin 2\tilde{\beta}_s$	$\sin 2(\tilde{\beta}_s + \tilde{\alpha}_d)$	$\sin 2(\beta - \beta')$

TABLE I. Values of $\text{Im}\lambda(B_q \rightarrow X)$ for the examples of the neutral B meson decay modes.

(1)–(4) correspond to four cases discussed in text. A zero indicates that the value is small, $\lesssim \mathcal{O}(10^{-2})$. The column indicated by “SM” shows the predictions in the SM [26].

VII. COMPATIBILITY WITH UPPER BOUND ON $\bar{\Theta}$; LOWER BOUNDS ON ELECTRIC DIPOLE MOMENTS.

It is interesting to estimate the *lower* bound on $\bar{\Theta}$ and hence on the neutron electric dipole moment d_n , for the different models.

First recall that in the standard model where the strong CP problem is unresolved - and requiring an additional mechanism such as the Peccei-Quinn symmetry [13] or a massless up quark (see, *e.g.* Ref. [14]) - there is no such lower limit because there is no reason to make $\bar{\Theta}$ small. If one simply puts the bare $\bar{\Theta}$ equal to zero (without motivation) then it has been pointed in Ellis and Gaillard [27] that there is a finite correction at two loops of $\sim 10^{-16}$ and an infinite renormalization at seven loops which is even smaller, $\sim 10^{-32}$ if one arbitrarily puts in a cut-off equal to the Planck mass. But these are not really predictions for a lower bound because there is fine-tuning unless there is an additional mechanism.

The value of $\bar{\Theta}$ is strongly constrained by the experiment of the neutron electric dipole moment; $\bar{\Theta} \leq 10^{-10}$. In the models considered in this paper the determinants of mass matrices of quarks are real, and the resultant $\bar{\Theta}$ is zero at tree level. However, it is generated at some loop level through corrections to the mass matrix; $\bar{\Theta} = \text{Im} \{ \text{tr} [M^{-1} \delta M] \}$, where M is the tree level mass matrix.

In the Aspon model a contribution to $\bar{\Theta}$ appears at one-loop level due to the mixing between the heavy scalar χ_I and the ordinary Higgs boson H given in Eq. (2.3) [9]. This contribution is estimated as [16]

$$\bar{\Theta} = \frac{\lambda x^2}{16\pi^2} , \tag{7.1}$$

where λ is an average value of λ_{IJ} in Eq. (2.3) and x is an average value of $|x_i|$ in Eq. (2.11). From a one-loop correction from the quark box diagram a lowest value of λ and hence $\bar{\Theta}$ are estimated as [17]

$$\lambda \gtrsim \frac{x^2}{16\pi^2} , \quad \bar{\Theta} \gtrsim \frac{x^4}{(16\pi^2)^2} . \tag{7.2}$$

This by using the upper bound of $\bar{\Theta}$ implies $x^2 \lesssim 10^{-3}$. When the Yukawa couplings are generation-independent, we obtain $\kappa \lesssim 3 \times 10^4 \text{ GeV}$ by combining this with the constraint (3.8) from ϵ_K . The assumption $\kappa > v$ gives the lower bound $x^2 \gtrsim 10^{-5}$, which leads to $\bar{\Theta} \gtrsim 4 \times 10^{-15}$, and hence $d_n \gtrsim 4 \times 10^{-30} \text{ e.cm.}$ As discussed in Section(V) one can admit $|C_{bd}^{(A)}|$ is as large as $|C_{bd}^{(\text{KM})}|$ by using the generation-dependent Yukawa couplings. In such a case the combination of Eqs. (7.2) with the constraint (5.2) from $B_d - \bar{B}_d$ mixing, we obtain $\kappa \lesssim 10^3 \text{ GeV}$ (rather than $\kappa \lesssim 3 \times 10^4 \text{ GeV}$). Equation (5.2) with the assumption $\kappa > v$ gives the lower bound $|x_1^* x_3| \gtrsim 2 \times 10^{-4}$, which combined with Eq. (7.2) leads $\bar{\Theta} \gtrsim 2 \times 10^{-12}$, and hence $d_n \gtrsim 2 \times 10^{-27} \text{ e.cm.}$

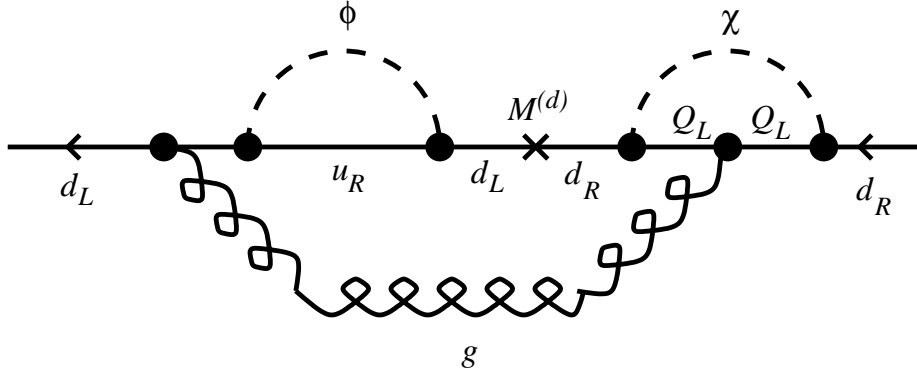


FIG. 4. Three loop diagram which gives a correction to the imaginary part of the d mass matrix in the model for Type R soft CP breaking.

In the model for Type R soft CP breaking the corrections to the imaginary part of the mass matrix of the down sector first arise at two-loop level, as pointed out in [6]. We estimate this as $\bar{\Theta} \simeq \lambda f^2 / (16\pi^2)^2$, where λ is an average value of λ_{IJ} in Eq. (2.3) and f is an average value of the Yukawa couplings. Different from the case of the Aspon model (where the top quark contributes), a lowest value of λ is here estimated from a one-loop correction from the box diagrams of *down-type* quarks. The resultant lowest value of $\bar{\Theta}$ is estimated as $\bar{\Theta} \gtrsim (f^4 / (16\pi^2)^3) \cdot (m_b / v)^2$, which leads only to $f^2 \lesssim 1$. This constraint is not strong. However, a stronger constraint comes from the three-loop diagram shown in Fig. 4. The correction from the diagram to the imaginary part of the mass matrix of down sector

is estimated as

$$\delta\mathcal{M}_d \sim \frac{\alpha_s}{4\pi} \frac{1}{16\pi^2 v^2} \frac{1}{16\pi^2} V^T (\mathcal{M}_u)^2 V \mathcal{M}_d X^I, \quad (7.3)$$

where $\alpha_s \simeq 0.12$ is the QCD coupling and V is a real orthogonal KM matrix. The contribution to $\bar{\Theta}$ is calculated by multiplying the above $\delta\mathcal{M}_d$ by $(\mathcal{M}_d)^{-1}$ and taking trace. Since \mathcal{M}_d is included between two hermitian matrices in $\delta\mathcal{M}_d$, enhancement factors arises from $(\mathcal{M}_d)^{-1}$. The resultant correction to $\bar{\Theta}$ is given by

$$\bar{\Theta}(\text{down}) \sim \frac{\alpha_s}{4\pi} \frac{m_t^2}{(16\pi^2)^2 v^2} \left[\frac{m_s}{m_d} V_{ts} V_{td} \text{Im} X_{12}^I + \frac{m_b}{m_d} V_{tb} V_{td} \text{Im} X_{13}^I + \frac{m_b}{m_s} V_{tb} V_{ts} \text{Im} X_{23}^I \right]. \quad (7.4)$$

By using $(m_d, m_s, m_b) \simeq (8, 150, 4800) \text{ MeV}$ and $(V_{td}, V_{ts}, V_{tb}) \simeq (5.9 \times 10^{-3}, 4.3 \times 10^{-2}, 1)$, the above expression becomes

$$\bar{\Theta}(\text{down}) \sim \left[9.0 \times 10^{-3} \text{Im} X_{sd}^I + 6.7 \text{Im} X_{bd}^I + 2.6 \text{Im} X_{bs}^I \right] \times 10^{-7}. \quad (7.5)$$

Then the constraint $\bar{\Theta} \lesssim 10^{-10}$ gives

$$\begin{aligned} |\text{Im} X_{sd}^I| &\lesssim 0.1, \\ |\text{Im} X_{bd}^I| &\lesssim 2 \times 10^{-4}, \\ |\text{Im} X_{bs}^I| &\lesssim 4 \times 10^{-4}. \end{aligned} \quad (7.6)$$

When we demand $|C_{bd}^{(R)}| \simeq |C_{bd}^{(\text{KM})}|$ consistently with the above upper bound, we need to require $|\text{Re} X_{bd}^I| \gg |\text{Im} X_{bd}^I|$. Then the bounds for M_Q and $\bar{\Theta}$ are same as those for the generation-independent Yukawa couplings. The combination of the upper bound (7.6) with the constraint obtained from ϵ_K (Eq. (3.9)) gives the upper bound for M_Q : $M_Q^{(R)} \lesssim 8 \times 10^4 \text{ GeV}$. The lower bound for $\bar{\Theta}$ may be obtained from the lower bound for \bar{X}_{sd} ($\bar{X}_{sd} \gtrsim 3 \times 10^{-4}$) derived from ϵ_K . The result is $\bar{\Theta} \gtrsim 3 \times 10^{-13}$, and hence $d_n \gtrsim 3 \times 10^{-28}$.

In the model of Type L soft CP breaking, a contribution to $\delta\mathcal{M}$ arises at two-loop level² from the diagram similar to the one for the Type R soft breaking model, while the

²This two-loop contribution is due to Sheldon Glashow.

three-loop diagram similar to the one in Fig. 4 does not contribute to $\bar{\Theta}$. So the dominant contribution to $\bar{\Theta}$ is estimated as $\bar{\Theta} \simeq \lambda f^2 / (16\pi^2)^2$. Similarly to the Aspon model, a lowest value of λ is estimated from a one-loop correction from the box diagram of *both* up-type *and* down-type quarks. The resultant value of $\bar{\Theta}$ is thus estimated as $\bar{\Theta} \gtrsim f^4 / (16\pi^2)^3$, which leads to $f^2 \lesssim 0.02$. For the case of generation-independent Yukawa couplings the combination of this upper bound with the constraint from ϵ_K gives an upper bound for M_Q : $M_Q \lesssim 2 \times 10^5 \text{ GeV}$. The bound $\bar{X}_{sd} \gtrsim 3 \times 10^{-4}$ leads to $\bar{\Theta} \gtrsim 2 \times 10^{-14}$, and hence $d_n \gtrsim 2 \times 10^{-29} \text{ e.cm.}$ On the other hand, when we require $|C_{bd}^{(L)}| \simeq |C_{bd}^{(\text{KM})}|$, the combination of $f^2 \lesssim 0.02$ with the constraint obtained from $B_d - \bar{B}_d$ mixing gives an upper bound for M_Q : $M_Q \lesssim 7 \times 10^2 \text{ GeV}$. A lower bound for \bar{X}_{bd} can be derived from the $B_d - \bar{B}_d$ mass difference (Section(V)): $\bar{X}_{bd} \gtrsim 7 \times 10^{-3}$, which leads to $f^2 \gtrsim 7 \times 10^{-3}$. From this lower bound the lower bound for $\bar{\Theta}$ is estimated as $\bar{\Theta} \gtrsim 10^{-11}$, and hence $d_n \gtrsim 10^{-26} \text{ e.cm.}$, quite close to the experimental limit.

VIII. SUMMARY OF PREDICTIONS.

The predictions of the different models we have studied are collected together³ are in Table II.

From this Table we see that the predictions for the different models are very divergent and therefore when the quantity (ϵ'/ϵ) is measured with an accuracy of 10^{-4} , and the CP asymmetry in $B \rightarrow \psi K_S$ is measured to determine whether or not $\sin 2\beta > 10^{-2}$ we will be able to exclude models. As mentioned in the Introduction we expect that both of these measurements will be completed within perhaps 2 or 3 years.

³In Table II the aspon model is “L-type spontaneous” meaning that light left-handed quarks couple to the new quarks. If we replace this by an aspon model with q= right-handed down-type quarks, the lower limits on λ and $\bar{\Theta}$ in Eq.(7.2) are each reduced by a factor $(m_b/v)^2 \sim 10^{-3}$.

	KM	R-type soft	L-type soft	Aspon
$\left(\frac{\epsilon'}{\epsilon}\right)$	few 10^{-4}	?	?	$< 10^{-5}$
Δ	big	flat	?	?
$\bar{\Theta}$	axion?	$> 10^{-13}$ (10^{-13})	$> 10^{-11}$ (10^{-14})	$> 10^{-12}$ (10^{-15})
d_n	10^{-32}	$> 10^{-28}$ (10^{-28})	$> 10^{-26}$ (10^{-29})	$> 10^{-27}$ (10^{-30})

TABLE II. Summary of results for the three CP violation models compared to the SM. Δ denotes the unitarity triangle determined from neutral B meson decays. A query ? denotes not *necessarily* pure superweak (essentially zero ϵ'/ϵ and a flat Δ), but becomes so if the Yukawa couplings are generation-independent. In that case, the first two rows in the last three columns become indistinguishable. Values in parentheses denote weaker bounds for the case of generation-independent Yukawa couplings, to be compared to generation-dependent ones.

ACKNOWLEDGEMENT

This work was supported in part by the US Department of energy under Grant No. DE-FG05-85ER-40219.

REFERENCES

- [1] S. Weinberg, Phys. Rev. Lett **31**, 657 (1976).
- [2] G.C. Branco, Phys. Rev. D **22**, 2961 (1980).
- [3] A.I. Sanda, Phys. Rev. D **23**, 2647 (1981); N.G. Deshpande, *ibid.*, 2654 (1981); J.F. Donoghue, B.R. Holstein and Y.-C. Lin, Nucl. Phys. B **277**, 650 (1981).
- [4] I.I. Bigi and A.I. Sanda, Phys. Rev. Lett. **58**, 1604 (1987); in “CP violation” ed. by C. Jarlskog; I.I. Bigi, A.I. Sanda and N.G. Uraltsev, in “Perspectives on Higgs Physics” ed. by G. Kane (World Scientific).
- [5] H.Y. Cheng, Int. J. Mod. Phys. A **7**, 1059 (1992); Y. Grossman and Y. Nir, Phys. Lett. B **313**, 126 (1993).
- [6] D. Bowser-Chao, D. Chang and W.-Y. Keung, Phys. Rev. Lett. **81**, 2028 (1998).
- [7] H. Georgi and S.L. Glashow, hep-ph/9807399 (unpublished).
- [8] P.H. Frampton and T.W. Kephart, Phys. Rev. Lett. **66**, 1666 (1991).
- [9] P.H. Frampton and D. Ng, Phys. Rev. D **43**, 3034 (1991).
- [10] A.W. Ackley, P.H. Frampton, B. Kayser and C.N. Leung, Phys. Rev. D **50**, 3560 (1994).
- [11] L. Bento, G.C. Branco and P.A. Parada, Phys. Lett. B **267**, 95 (1991); G.C. Branco, T. Morozumi, P.A. Parada and M.N. Rebelo, Phys. Rev. D **48**, 1167 (1993).
- [12] M. Kobayashi and T. Maskawa, Prog. Theor. Phys. **49**, 652 (1973).
- [13] R.D. Peccei and H.R. Quinn, Phys. Rev. Lett. **38**, 1440 (1977); Phys. Rev. D **16**, 1791 (1977).
- [14] R.D. Peccei, in “CP violation” ed. by C. Jarlskog; and references therein.
- [15] T. Inami and C.S. Lim, Prog. Theor. Phys. **65**, 297 (1981).

- [16] P.H. Frampton and S.L. Glashow, Phys. Rev. D **55**, 1691 (1997).
- [17] P.H. Frampton and M. Harada, UNC-Chapel Hill Report IFP-759-UNC (1998) *hep-ph/9805489* (to appear in Phys. Lett. B).
- [18] A.J. Buras, M. Jamin and M.E. Lautenbacher, Phys. Lett. B **389**, 749 (1996); M. Ciuchini, Nucl. Phys. B, Proc. Suppl. **59**, 149 (1997); M. Ciuchini, E. Franco, G. Martinelli, L. Reina and L. Silvestrini, Z. Phys. **C68**, 239 (1995); S. Bertolini, M. Fabbrichesi and J.O. Eeg, hep-ph/9802405; S. Bertolini, J.O. Eeg, M. Fabbrichesi and E.I. Lashin, Nucl. Phys. **B514**, 63, 93 (1998).
- [19] A.J. Buras, M. Jamin and M.E. Lautenbacher, Phys. Lett. B **389**, 749 (1996).
- [20] G. Buchalla, A.J. Buras and M.K. Harlander, Nucl. Phys. B **337**, 313 (1990).
- [21] G. Buchalla, A.J. Buras and M.E. Lautenbacher, Rev. Mod. Phys. **68**, 1125 (1996).
- [22] P.H. Frampton and M. Harada, UNC-Chapel Hill Report IFP-757-UNC (1998) *hep-ph/9803416* (to appear in Phys. Rev. D).
- [23] R. Barbieri, L. Hall, A. Stocchi and N. Weiner, Phys. Lett. B **425**, 119 (1998).
- [24] S. Mele, hep-ph/9808411 (unpublished); hep-ph/9810333 (unpublished).
- [25] J. P. Silva and L. Wolfenstein, Phys. Rev. **D55**, 5331 (1997).
- [26] M. Neubert, Int. Jour. Mod. Phys. A **11**, 4173 (1996).
- [27] J. Ellis and M.K. Gaillard, Nucl Phys, **B150**, 141 (1979).